

*Chapter 2***POPULATION DENSITY CONTROL IN SYNTHETIC BACTERIAL COMMUNITIES****2.1 Introduction**

Microbial communities are everywhere and perform critical functions for the health of ecosystems at every scale. When environments change, community species compositions change, but we cannot predict changes or prevent them without greater knowledge of microbial communities and community control technology.

Bioengineers in various fields recognize the importance of microbial community control for different reasons. Synthetic biologists run into limits on the complexity of genetic circuits that are tolerated by homogeneous populations of microbes; increasing the complexity of genetic circuits requires the distribution of circuit burden across a heterogeneous community of microbes [41, 42]. Additionally, genetic circuits designed without provisions for coordination of circuit-containing cells lose precision in their function due to cell-to-cell variability [43, 44]. Control of community composition and gene expression dynamics are required to create a stable platform for reliable circuit function.

Bioprocess engineers recognize the efficiency and yield gains to be made by distributing production processes across a community of organisms [45, 46]. Literature detailing the benefits of polyculture production emphasizes that this process is optimized at specific community compositions, necessitating precise, stable control of community composition [47–49].

Ecologists and microbiologists recognize the potential of microbial community control to enable greater understanding of biological diversity through community control experiments mimicking and investigating natural ecology. Those seeking to remediate and preserve natural microbial diversity see the value of genetic circuits for community control in efforts to understand and beneficially alter natural microbial communities [50, 51].

At its core, control of community composition is really the control of population density for many coexisting microbes at the same time. The basic unit of multi-member composition control is control of an individual homogeneous population's

density. The population density control circuit published by You *et al* [52] is one of the foundational genetic circuits in the population control space; it has served as template, springboard and inspiration for studies building alternative or more complex population control circuits.

Despite the clear utility of genetic circuits that explicitly control population sizes, a relatively small number of circuits tackling this challenge have been published in the space of community synthetic biology.

In You *et al* [52], the authors create a genetic circuit closely mimicking the architecture of native autoinducing quorum sensing circuits, but replace the induced downstream gene with the *ccdB* toxin (Fig 1B in [52]). Instead of coordinating expression of a bioluminescent protein with the quorum sensing chemical (as in *Aliivibrio fischeri* [53]), this circuit coordinates cell death throughout a population of *E. coli*, capping normal population growth at a specific density. The components of the circuit are the LuxI AHL synthase, LuxR activatory transcription factor, pLux inducible promoter and *ccdB* toxin.

With rare exceptions, other genetic circuits designed for population control are similarly designed, using quorum sensing mediated autoactivation of toxins or growth inhibitors to affect bacterial population growth.

In Scott *et al*'s multi-strain community circuit [54], culture dominance by one strain is avoided by the expression of a very similar quorum sensing autoactivation circuit in each strain. The Lux or Rpa systems (in the two community member strains) coordinate expression of the $\phi X174$ lysis protein, causing each strain's population to grow up to a threshold density, at which point the quorum sensing signal activates lysis throughout the population, dramatically reducing strain density. Oscillatory cycles of growth and lysis of the two strains in coculture allow cocultures that would ordinarily become dominated by one strain to maintain a mixed composition over long culture times. Where the You *et al* population control circuit sets steady state population densities, the Scott *et al* circuit produces oscillatory population dynamics (although a steady state is possible in specific parameter ranges). This difference in circuit behavior is not likely to be caused by the difference in toxic protein (*ccdB* vs $\phi X174$), but rather due to the positive feedback regulation of AHL production in Scott *et al*, compared to the externally-inducible, but stable rate of AHL production in You *et al*.

With a similar goal of maintaining coculture diversity, Dinh *et al* created a feedback

AHL regulated circuit for control of bacterial *growth* rather than *death* [55]. In this circuit, growth rate of one strain in coculture is regulated by the degradation of phosphofructokinase A (*pfkA*) in response to Lux AHL. In this way, even when this strain dominates a coculture at inoculation, over time its growth rate decreases and allows a second uncontrolled strain to grow, maintaining a mixed population. The growth control circuit is structured identically to the You *et al* circuit but uses a growth inhibitory mechanism rather than a death activatory toxin. Despite stable AHL production rates in this circuit, the choice to inhibit *growth* with AHL feedback does not produce a steady population density, presumably because *pfkA* is never completely degraded away and cells may continue to grow even at high population densities. Contrast this with the expression of a toxin, which can theoretically increase the death rate in a population to match the growth rate, thereby allowing a steady state population to be achieved.

Quorum sensing and growth or death regulation are not the only components that can be used to regulate population densities. Kerner *et al* created a coculture of auxotrophic *E. coli* whose growth rate and composition can be precisely tuned by the expression of metabolite export proteins [15]. In this case, metabolites play the dual role of intercellular signal and growth regulator, where AHLs and toxins are used together in other circuits. The sub-populations in this community cannot be separated from each other; their genetic circuits cannot perform monoculture population density control because by nature, auxotrophs are dependent on partners or external supplementation for survival.

Other chemicals and proteins can be used as combined signals and growth regulators. Antibiotics and their resistance genes can regulate growth and death in genetic circuit designs, as can secreted intercellular bacteriocin toxins like nisin or lactococcin A [56, 57].

Returning to AHL and toxin-based genetic circuits, more complexity is possible in genetic circuit function. Balagaddé *et al* used the *ccdA* antotoxin in conjunction with *ccdB* to create a genetic circuit capable of downregulating population density with the *ccdB* toxin *and* inhibiting that downregulation with *ccdA* (rescuing a population from growth inhibition). Using this new circuit function, they designed a synthetic predator-prey ecology capable of recapitulating the out of phase oscillations characteristic of that relationship [58].

These different circuits illustrate the various ways population regulation can be approached using genetic circuit parts appropriated from bacterial physiology. There

remains design space to be filled in *stable* monoculture population density control by the combination of the technologies reviewed above. By adding the *ccdA* antitoxin to the population capping architecture published by You *et al.*, we create a genetic circuit capable of stable population control with the additional functionality afforded by antitoxins. This circuit allows the stable capping of population density using feedback toxin expression, but also the progressive release of a population density cap with independently regulated antitoxin expression, allowing two-input upward and downward control of population density.

Using a functional screening process, we build an implementation of the *cap and release* circuit. Then, by adding quorum sensing signal degradation, we give experimenters control over AHL degradation, a critical parameter in circuit function. The resulting signal degradation-capable *cap and release* circuit is an environment-independent controller of population density as well as a scalable motif for single and multiple strain community control.

2.2 Results

Examining a feedback population control circuit

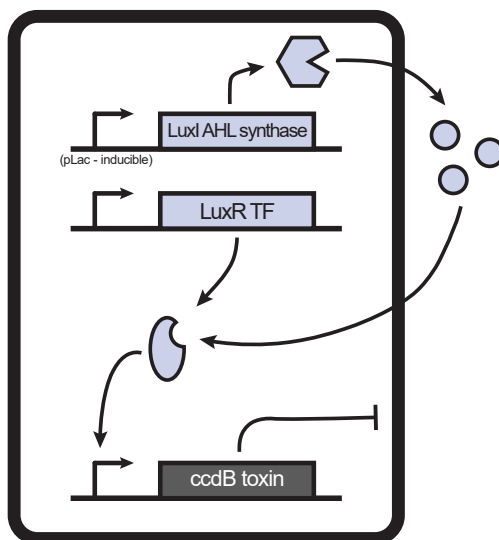


Figure 2.1: Architecture of *pop cap* Schematic representation of the population capping circuit published in [52]. Secreted AHL signals implements negative feedback control of population density.

We started by reexamining the design of the You *et al.* (2004) population control circuit (Fig. 2.1). The *pop cap* design is based on the production, sensing and response to secreted acyl-homoserine lactone (AHL) quorum sensing molecules that

broadcast population density throughout the community. Cells respond to AHL by expressing a toxin, killing themselves when AHL and toxin levels get too high. This negative feedback causes the artificial capping of the population's density below normal limits (normal e.g. nutrient limitation or maximum physiologic density causing stationary phase). For its population capping function, we call this the *pop cap* circuit

The specific components that make up the You *et al.* *pop cap* implementation (and much of our later circuit designs) are as follows:

- **pLac inducible promoter:** An inducible promoter repurposed from its native role in the *Lac* operon. Transcription from this promoter is activated by the unbinding of the LacI repressor when LacI is complexed with lactose, or in this case, the modified inducer chemical IPTG (isopropyl β -D-1-thiogalactopyranoside). In this circuit, pLac drives LuxI expression.
- **LuxI AHL synthase:** An enzyme that synthesizes Lux-type AHL chemicals (3-oxohexanoyl-homoserine lactone, 3-O-C6-HSL) from S-adenosylmethionine (SAM) (amino donor) and an appropriate acyl–acyl carrier protein (acyl-ACP) (acyl donor) [59]. Lux AHL chemicals can freely diffuse through bacterial membranes, meaning their concentration in a mixed culture environment is equal both inside and outside cells.
- **LuxR transcription factor:** A transcription factor that binds Lux AHL molecules, dimerizes, then binds as a dimer-AHL complex to the pLux promoter, *activating* transcription of downstream genes.
- **ccdB toxin:** A small 101 amino acid toxin protein expressed natively from the *E. coli* F plasmid *ccd* operon. In this circuit, its transcription is driven by the pLux inducible promoter. ccdB covalently traps DNA gyrase in an unstable DNA strand-cleaved conformation [60, 61]. Stuck in this state during replication, the genome fragments and the cell dies

Stripping away the minutiae of the circuit's implementation in You *et al.* (exact plasmid origins of replication, promoter types, plasmid design) we can write a set of differential equations that describe the major kinetic events that underlie the circuit's activity. The dynamics of C , cell population size (ml^{-1}); T , average intracellular ccdB toxin concentration (nM); and A , AHL chemical concentration (nM) are described by the following:

$$\frac{dC}{dt} = k_C C \left(1 - \frac{C}{C_{max}}\right) - d_C C T, \quad (2.1)$$

$$\frac{dT}{dt} = k_T A - d_T T, \quad (2.2)$$

$$\frac{dA}{dt} = k_A C - d_A A. \quad (2.3)$$

We assume in eq. (2.1) that population (C) growth unconstrained by circuit action follows a logistic model with a growth rate of k_C (h^{-1}), a carrying capacity of C_{max} (ml^{-1}), and an intrinsic death rate of D (h^{-1}). During circuit-regulated growth, we assume the cell death rate is proportional to the intracellular concentration of the toxin protein (T) with a rate constant of d_C ($nM^{-1}h^{-1}$). In eq. (2.2) we assume the production rate of toxin T is proportional to an activatory Hill function of AHL concentration (A , assumed to be the same inside and outside the cells due to free transmembrane diffusion) with a rate constant of k_T (h^{-1}), equilibrium constant of k (nM), and Hill coefficient β (assumed to be 2). Toxin is produced from a promoter activated by a complex of AHL chemical and dimerized AHL transcription factor, commonly expressed as a Hill function, as we do here. In eq. (2.3) we assume AHL signal synthesis rate is proportional to C with a rate constant of k_A ($nMmlh^{-1}$); in the laboratory implementation of this circuit, k_A is modifiable by the experimenter by changing the concentration of the IPTG inducer of pLac. We also assume degradation of toxin and AHL follows first-order kinetics with rate constants of d_T (h^{-1}) and d_A (h^{-1}).

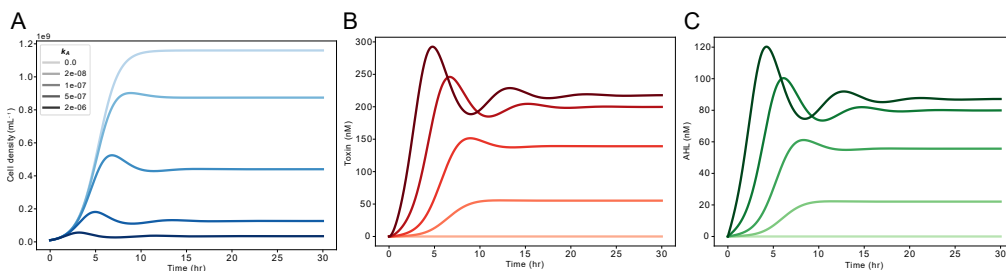


Figure 2.2: Simulation of *pop cap* system Dynamics of each species in the model of *pop cap* are simulated in response to increasing AHL production rate, k_A . (A) Total population density (B) Average intracellular toxin concentration in the population. (C) Environmental concentration of AHL, assumed to be equal inside and outside cells due to free diffusion.

Simulations of the model demonstrate the expected behavior of the system (see materials and methods for parameters and initial conditions) (Fig. 2.2). In each

panel, we have simulated the dynamics of each species using five different values for k_A (simulating response to IPTG inducer). With k_A at 0, the circuit is "OFF" and the model predicts normal logistic growth of the cell population to C_{max} . With increasing k_A , population growth overlaps normal logistic growth, but eventually deviates, overshoots its final steady state, then finally settles at steady state at a density below C_{max} . This is the population capping function of the circuit. Population capping is mediated by the *ccdB* toxin, induced by AHL signal produced by the population. The *ccdB* toxin and AHL signal accumulate to higher and higher steady state concentrations with increasing k_A , depressing the population density steady state with increasing *ccdB* concentration (Fig. 2.2, B-C).

Demonstrating population control

The You *et al.* implementation of *pop cap* uses secreted Lux-type (3-oxohexanoyl-homoserine lactone, 3-O-C6-HSL) quorum sensing molecules to broadcast population density and the *ccdB* toxin to kill cells. The LuxI AHL synthase is expressed by the inducible pLac promoter, responsive to IPTG. The plasmids that carry the circuit are structured as follows:

- **Plasmid 1:** ColE1 origin (high copy ~300-500/cell [62, 63]), pLac promoter drives the *co-transcriptional* expression of both the LuxR TF and LuxI synthase.
- **Plasmid 2:** p15a origin (low copy ~10-15/cell), pLux promoter drives expression of *ccdB* toxin fused to *lacZ α* fragment.

Notably, the *ccdB* expressing Plasmid 2 has copy number ~200-400x lower than that of Plasmid 1. All genetic constructs "leak" a small amount of protein even without induction of transcription; it is possible that, due to the potency of *ccdB*, using anything other than a low copy plasmid may amplify *ccdB* leak to lethal levels, even in the absence of Lux AHL chemical. Plasmid 1 (pLuxRI2 from You *et al.*) transcribes the coding sequences of LuxI and LuxR together, meaning an experimenter increases the amount of transcription factor in a cell while they increase Lux AHL synthesis rate. This produces protein dynamics not captured in the mathematical model; it is possible that the Hill equation assumptions made about *ccdB* toxin expression in response to Lux AHL, via LuxR, are not always accurate if the LuxR concentration changes along with AHL concentrations.

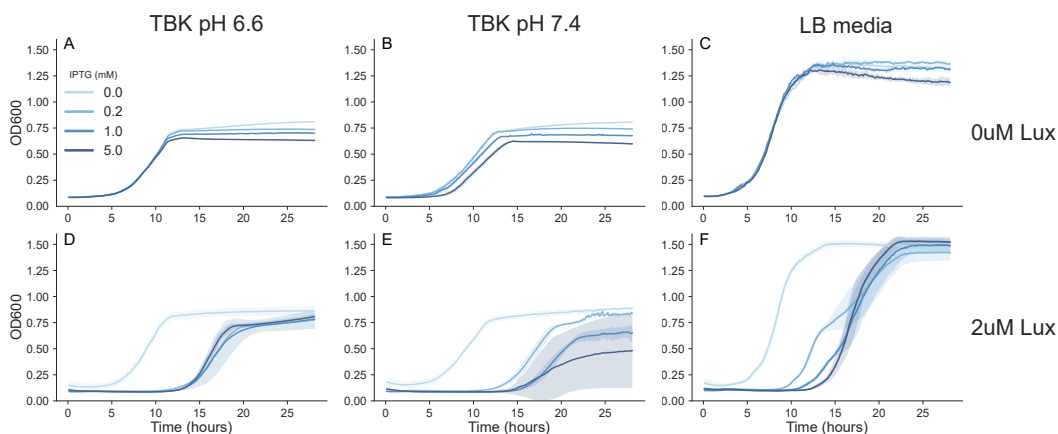


Figure 2.3: Recapitulating population capping. Cells containing the *pop cap* circuit were grown in the indicated media and inducer concentrations. Curves are the mean of 3 replicates, shaded areas represent standard deviation.

We tested the *pop cap* circuit using the original plasmids (*plasmid 1*: pLuxRI2 and *plasmid 2*: *pluxccdB3*) in DH5 α *E. coli*. Cultures were grown in 4 concentrations of IPTG (mimicking 4 increasing k_A values) in three different growth media: the buffered defined TBK medium from the You *et al* publication at two pHs and standard LB medium.

Pop cap - TBK pH 6.6	OD600 - endpoint	σ
Uninduced maximum density	0.8106	0.0035
5 mM IPTG - cap	0.6316 (77% uncapped)	0.0058
Pop cap - TBK pH 7.4		
Uninduced maximum density	0.807	0.001
5 mM IPTG - cap	0.599 (74% uncapped)	0.0075
Pop cap - LB		
Uninduced maximum density	1.319	0.039
5 mM IPTG - cap	1.19 (90% uncapped)	0.038

In the TBK media (Fig. 2.3, panels A-B), our experiments consistently recapitulated the qualitative function of the circuit, but never matched the published magnitude of the circuit's effect. You *et al.* demonstrated population density capping to 10% the density of a control population (hereafter referred to as "max density") with 1 mM IPTG induction, while our experiments only produced a cap to ~75% of max density at 5 mM IPTG. Between the two TBK media at different pH values, the circuit had very similar population capping performance, but growth dynamics were significantly different. In TBK at pH 6.6, growth rate in each IPTG concentration was nearly identical until 10 hours, at which point each culture abruptly stopped

growing at its population cap.

Similar abrupt halts in growth were observed in TBK pH 7.4, but each culture's growth rate was different, producing non-overlapping curves. Growth at pH 6.6 more closely recapitulated the model's prediction that capped populations would grow similarly to the uncapped population until an abrupt decrease in growth rate; at pH 7.4, IPTG induction produced a noticeable difference in growth rate between the capped cultures.

In LB medium (Fig. 2.3, panel C), circuit induction had an even smaller effect on population density; no difference in density between the IPTG concentrations was apparent until after 11 hours, when the culture in 5 mM IPTG slightly decreased in density until it settled only 10% lower by the end of the experiment.

While these data suggested the dynamic range of the circuit was limited, we demonstrated the full potential dynamic range of the circuit by progressively inducing circuit components with IPTG in the presence of 2 μ M Lux AHL. In all media, induction of circuit components with IPTG combined with manual addition of Lux AHL (rather than relying on LuxI AHL synthesis) produced dramatic population caps (Fig. 2.3, panels D-F). The intensity of these caps was such that no growth was observed in any condition except the uninduced 0 mM IPTG condition, in which the cells would not be expected to respond to the high concentration of Lux AHL.

These heavily capped cultures did not grow from their seeding densities until 10-12 hours after the start of the experiment. At that time, each heavily capped culture began to overgrow its cap until it reached the vessel's capacity. In TBK pH 6.6, all heavily capped cultures all began to grow after 12 hours, following approximately normal logistic growth to maximum density by the end of the experiment. In TBK pH 7.4 and LB medium, the time at which the capped culture began to grow was related to the IPTG inducer concentration. With increasing IPTG induction, the capped culture remained dormant at its seeded density for longer times.

These results suggested that this implementation of the circuit was not optimized for maximum response, especially not in LB medium. An improperly low Lux AHL production rate seems a probable cause of this poor dynamic range given how drastic an effect exogenous AHL could produce when the circuit response elements were induced with IPTG. Additionally, we found that heavily capped cultures were not stable; rather, they would eventually overgrow their very low population cap and continue growing to maximum density. This suggests either an evolutionary escape

from population control [64], or unforeseen dynamics in circuit components (e.g. unexpected decrease in AHL signal concentrations or *ccdB* production). We believe this phenomenon is caused by the growth of cheater bacteria who have evolved away from circuit function. Sequencing the plasmids of the overgrown cultures may reveal inactivating changes in plasmid sequence.

It is important to note that our data were taken using optical density (OD600) absorbance measurements, while the original authors measured viable colony forming units (CFU). Our results may have been identical in magnitude to those published, but were obscured by the different measurement technique. The toxic mechanism of *ccdB* may affect these measurement types differently. We address this in the following section.

Toxin sequestration allows population cap release—the *cap and release* motif

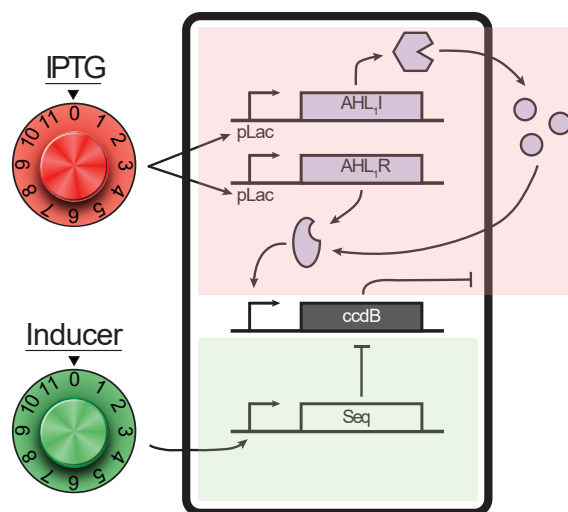


Figure 2.4: The *cap and release* circuit motif. Red shaded area indicates the feedback populating *capping* arm of the circuit. Green shaded area indicates the *cap release* arm. Seq is either the *ccdA* antitoxin that sequesters *ccdB* at the protein level, or RNA-OUT, which binds the RNA-IN sequence on *ccdB* mRNA, sequestering it at the mRNA level.

The *ccdB* toxin has a naturally occurring peptide antitoxin, *ccdA*, that is involved in regulating the *ccd* operon, from which both *ccdB* and *ccdA* are expressed [65, 66]. By creating a third *ccdA* expressing plasmid to accompany the 2 *pop cap* plasmids, we modified the *pop cap* system to include experimenter-controlled *ccdB* toxin sequestration. This sequestration mechanism acts at the *protein level*; *ccdB* and *ccdA* are both proteins that sequester each other.

- **ccdA antitoxin:** When present together with *ccdB*, *ccdA* binds *ccdB* with

picomolar affinity [67], sequestering it and blocking its toxic activity. *ccdA* can bind and inactivate both free *ccdB* and *ccdB* already complexed with DNA gyrase; *ccdA* reverses *ccdB*/gyrase binding and restores gyrase to normal function.

We also designed an alternate version of the *pop cap* architecture containing a different *ccdB* sequestration device, this one using the Rhl AHL system [68] and an mRNA level sequestration system called RNA-IN/RNA-OUT [69] to regulate expression of the *ccdB* toxin. This mechanism acts at the mRNA level:

- **RNA-IN:** An RNA sequence containing a ribosome binding site (RBS) that initiates translation of the downstream encoded protein. The RBS is normally accessible to ribosomes (i.e. it is not hidden from ribosomes by any secondary RNA structure). RNA-IN is built into genetic circuits as a DNA sequence between a promoter and protein coding sequence; it becomes functional when transcribed into RNA.
- **RNA-OUT:** The sequestration device for the RNA-IN containing mRNA. It is also built into circuits as a DNA sequence that becomes a functional mRNA sequence when transcribed from a promoter. RNA-OUT binds to a section of RNA-IN via RNA base pairing, causing a conformation change in the IN/OUT complex that hides the RBS in RNA-IN from ribosomes, blocking translation of the gene downstream of RNA-IN.

By adding a *ccdB* sequestration device (either *ccdA* or RNA-OUT) to the *pop cap* circuit under regulation by a second external inducer, we turned the *pop cap* circuit into a new circuit motif with two inputs. As demonstrated above, feedback control of *ccdB* expression via AHL signals sets a steady state population cap. Inducible *ccdB* sequestration allows the progressive release of that population cap. We call this motif the ***cap and release*** circuit (Fig. 2.4). We add a new equation to the *pop cap* model to reflect the new circuit components.

$$\frac{dC}{dt} = k_C C \left(1 - \frac{C}{C_{max}}\right) - d_C C T, \quad (2.4)$$

$$\frac{dT}{dt} = k_T A - k_{on} T R - d_T T, \quad (2.5)$$

$$\frac{dR}{dt} = g_R - k_{on} T R - d_R R, \quad (2.6)$$

$$\frac{dA}{dt} = k_A C - d_A A. \quad (2.7)$$

Where R (nM) represents the average concentration of sequestration device in the population.

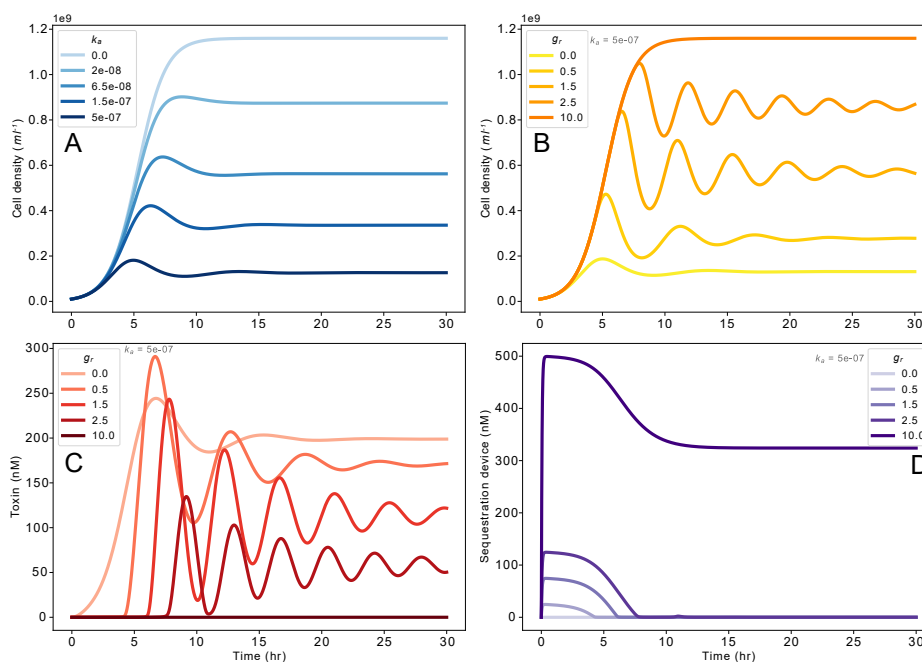


Figure 2.5: Simulation of *cap* and *release* system Population dynamics of *cap* and *release* are simulated in response to (A) increasing AHL production rate, k_A , (B) increasing *Seq* production rate, g_R , against a background of high k_A . (C) Toxin dynamics during *cap* release with increasing g_R . (D) *Seq* dynamics during *cap* release with increasing g_R .

Equations (2.4) and (2.7) are unchanged from the *pop cap* model (eqs. (2.1) and (2.3)). We have added eq. (2.6) that models the production of the toxin sequestration device (*Seq*). We lump all terms related to *Seq* production into g_R (nMh^{-1}), as this term is arbitrarily modifiable by the experimenter by changing *Seq* inducer concentration. Toxin/*Seq* binding is assumed to be proportional to their

concentrations with constant k_{on} ($nM^{-1}hr^{-1}$). We omit an unbinding term since the affinity between toxin and *Seq* is incredibly strong for both systems used. *Seq* degradation is first-order with rate d_R (hr^{-1}). The same toxin/*Seq* binding term is added to eq. (2.2) to form eq. (2.5). Now, cell death is modified only by *free* toxin, since the sequestration complex is inert.

Simulating the responses of this system to increasing k_A (simulating increasing IPTG inducer concentration) (Fig. 2.5, A) and g_R (increasing *Seq* inducer concentration) (Fig. 2.5, B-D), demonstrates both population control behaviors of this circuit. As in *pop cap*, increasing k_A alters normal logistic growth to produce population density steady states lower than maximal. Increasing g_R against a background of high k_A increases the amount of *Seq* present in each cell, which sequesters an approximately equal concentration of ccdB toxin, releasing population capping pressure and producing higher steady state population density. We see this clearly in (Fig. 2.5, D) in which increasing amounts of *Seq* are produced in the population, but as ccdB toxin is produced, free *Seq* concentration decreases to zero if more ccdB is produced than *Seq*, or to a positive steady state value if more *Seq* is produced than ccdB. When excess *Seq* is produced due to very high g_R , growth is normal because no free toxin exists to limit growth.

Scanning the parameters associated with *Seq*: g_R , k_{on} , and d_R , we find that g_R must be large (100-1000x larger than k_T) to make significant changes to population density; that k_{on} must also be large to allow toxin sequestration to occur at a useful rate; and that d_R should also be large relative to d_T to avoid extremely oscillatory toxin and population dynamics during cap release that may preclude establishment of a population steady state in a normal experiment duration (10-24 hours). By design or by nature, all of these parameter values are captured in our circuit design. *Seq* is expressed from a promoter-RBS combination much stronger than that expressing ccdB toxin *and* this stronger *Seq* expression unit is contained on a plasmid with copy number $\sim 100x$ larger than the ccdB expression plasmid. These two factors satisfy the need for larger g_R than k_T . By nature, both ccdA and RNA-OUT *Seq* devices have extremely high affinity for ccdB (or its mRNA) and significantly faster d_R relative to d_T , satisfying the requirements for useful and timely *Seq* activity. It is a well-known feature of the native ccdA/ccdB system that ccdA is degraded much faster than ccdB [70]. The half-life of mRNA is also significantly shorter than that of protein [71].

Circuit component sequestration is a tool used for a number of reasons in recent

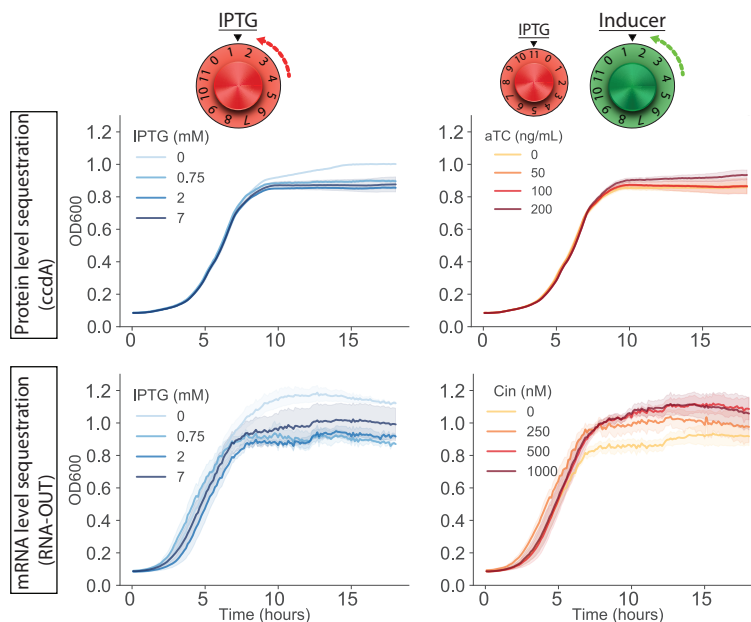


Figure 2.6: Testing toxin sequestration. Both mRNA and protein-level *ccdB* sequestration modules were tested in two different *cap and release* circuit implementations. (LEFT column) - Population capping with IPTG. (RIGHT column) - Release from population capping at 7 mM IPTG. Rows correspond to the two circuit implementations with different sequestration modules.

synthetic biology literature. Circuits with two functional sequestering elements allow the closest biological approximation of an integral controller [72, 73]. While circuits built using the *cap and release* motif do not work around the hurdle of species dilution and degradation [74], *ccdB* sequestration does allow for improved control accuracy if either species or the complex is used to regulate controller output, as we do in this circuit with unbound *ccdB*. Sequestration in the *cap and release* system gives an experimenter both downward and upward control over a community's population density with independent inputs, creating opportunities to translate information from two signals into complex density regulation. The two-input motif can also be configured to link different strains together to form a controlled multi-membered community.

We grew cultures expressing both *cap and release* circuit variants (employing either *ccdB/A* protein sequestration or RNA-IN/RNA-OUT mRNA sequestration) in TBK medium pH 6.6.

In the *ccdB/ccdA* variant (Fig. 2.6, TOP row), population capping was again only modest, to 83% the density of uninduced culture. Similar to our test of *pop cap*, cultures at all IPTG concentrations grew identically until around 8 hours, at which

point they abruptly ceased growth and remained stable at their population cap. The growth rate of *uninduced* culture slowed at this time, but did not stop, continuing slowly until it reached its maximum by the end of the experiment. Population capped at 7 mM IPTG, the *ccdB/ccdA* variant was very slightly released from its population cap by *ccdA* induction with aTC; maximal *ccdA* induction did not fully release the population cap to the density achieved by uninduced culture.

<i>Cap and release - ccdB/ccdA</i>	OD600 - endpoint	σ
Uninduced maximum density	1.001	0.001
7 mM IPTG - cap	0.836	0.041
200 ng/mL aTC - release	0.934	0.031

The variant employing mRNA sequestration (Fig. 2.6, BOTTOM row) demonstrated similar population capping in response to IPTG. Interestingly, the maximal 7 mM IPTG condition produced *less* of a population cap than did lower concentrations. The strongest population cap was produced by 0.75 mM IPTG to 77.5% of uninduced density. Induction of mRNA sequestration with Cin AHL against 7 mM IPTG produced intermediate amounts of population cap release, culminating in nearly complete cap release with 1mM Cin.

<i>Cap and release - RNA-IN/RNA-OUT</i>	OD600 - endpoint	σ
Uninduced maximum density	1.121	0.009
0.75 mM IPTG - cap	0.869	0.0015
7 mM IPTG - cap (less effective)	0.904	0.03
1 mM Cin - release (from 7 mM IPTG)	1.058	0.1

Comparing the two circuit variants, approximately similar population capping (to about 80% of max density) was achieved by both, *but* more complete cap release was observed in the variant employing RNA-level toxin sequestration (RNA-OUT) (Fig. 2.6). Induction of *ccdA* only released the population cap back to 93% maximum density, while RNA-OUT completely removed the cap.

The growth dynamics of each population may be affected by the sequestration device used to modify *ccdB* levels. In the variant with protein-level sequestration (*ccdA*, Fig. 2.6 TOP row), growth of each population is smooth and consistent across replicates. In the variant employing RNA-level sequestration (RNA-IN/OUT, Fig. 2.6 BOTTOM row), growth of each population is jerky and noisy across replicates. We hypothesize that the molecular level (DNA, RNA, protein) of *ccdB* sequestration is responsible for these effects; at lower mRNA copy numbers compared to protein

copy numbers, stochasticity in sequestration may play a larger role in regulating *ccdB* activity, producing the observed noise and variability in cell growth.

In a similar experiment testing the *ccdB/ccdA* sequestration *cap and release* variant, we were able to compare methods of population density measurement. In this experiment, 5 mM IPTG and 100 ng/mL aTC were the highest concentration of population cap and release inducer used, respectively. At the end of the experiment presented in Fig. 2.12, we removed samples of protein-level sequestration (*ccdB/ccdA*) circuit cultures and used two different methods to determine the number of viable cells present: traditional petri plate CFU counting or a small volume culture spotting technique (see materials and methods). We clearly find that absorbance-based optical density measurements overestimate the number of viable cells present in culture compared to CFU counts (Fig. 2.7). OD600 measurements normalized to the uninduced growth condition indicate population capping to 84% uninduced density with 5 mM IPTG. Maximal *ccdA* induction at 100 ng/mL aTC produced an apparent complete recovery of population density with OD600 measurement.

Both methods of viable cell counting reveal significantly stronger population capping to normalized values between 25-50% of uninduced population density with maximal 5 mM IPTG induction. 100 ng/mL aTC induction of *ccdA* is revealed to release these strong population caps only about halfway back to maximum density rather than the complete recovery reported by OD measurement. The viable cell counts from these populations tell us that our experiments approximate the originally published population capping magnitude more closely than optical density measurements report, but we still have not replicated capping to $\leq 10\%$ of max population density.

The specific mechanism of action of *ccdB* may be responsible for the inflation of

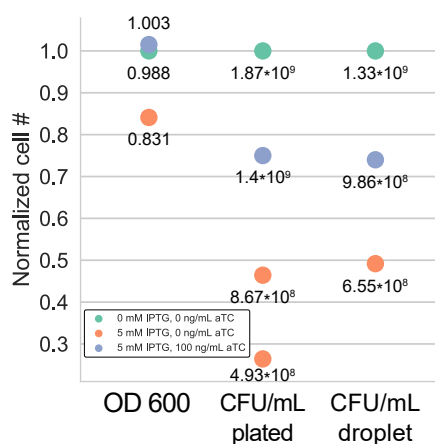


Figure 2.7: Comparing absorbance and viable cell counting methods. Values for each column are normalized to the uncapped condition. Densities are those after 18 hours of growth. Absorbance based optical density clearly overestimates the viable cell count in a culture undergoing capping with the *ccdB* protein.

absorbance-based measurement compared to viable cell counts. It traps DNA gyrase in an unstable DNA strand-cleaved conformation [60, 61]. Stuck in this state during replication, the genome fragments and the cell dies. A cell without a genome may still look alive to an absorbance-based measuring device when it is more or less a husk of a cell that will not *act* alive when checked for viability.

Experimenter-controlled signal degradation and an optimized *cap and release* motif

In their characterization of *pop cap* the authors modified passive degradation rates of the Lux AHL signal by varying experiment pH, showing that higher degradation rates at higher pH result in lower steady state AHL concentrations and thus, higher steady state population density [52]. While increasing pH will increase the passive degradation of AHL signals, not every environment—especially inaccessible field environments—may support appropriate AHL degradation parameters. To make the circuit environment-independent, we added inducible expression of the *aiiA* lactonase, a promiscuous degradase of AHL signals (Fig. 2.8).

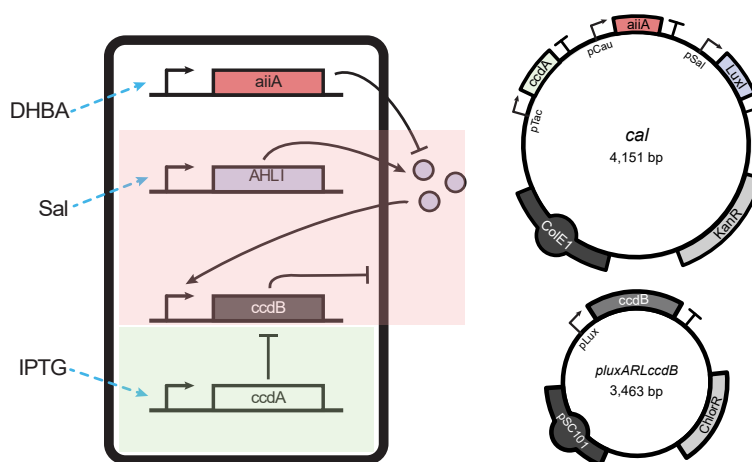


Figure 2.8: The "cap and release" population control motif. (A) Diagram of circuit components. Sal = sodium salicylate, DHBA = 3,4-dihydroxybenzoic acid, IPTG = isopropyl β -D-1-thiogalactopyranoside. AHL₁ is Lux (3-O-C6-HSL) AHL. (B) Plasmid design. *ccdB* is expressed from a separate very low copy plasmid (pSC101 approx. 5 per cell). All other plasmids expressed together from a high copy plasmid (ColE1 approx. 300-500 per cell). Cell line used expresses all TFs including LuxR from genome [34].

- ***aiiA* lactonase:** A protein originally discovered in *Bacillus thuringiensis*. It is a metalloenzyme capable of hydrolyzing the lactone ring of AHL molecules. Its expression by *B. thuringiensis* in various environments has been shown

to attenuate virulence of pathogenic bacteria that rely on AHL signals for community coordination. [18, 75, 76]

$$\frac{dC}{dt} = k_C C \left(1 - \frac{C}{C_{max}}\right) - d_C C T, \quad (2.8)$$

$$\frac{dT}{dt} = k_T A - k_{on} T R - d_T T, \quad (2.9)$$

$$\frac{dR}{dt} = g_R - k_{on} T R - d_R R, \quad (2.10)$$

$$\frac{dA}{dt} = k_A C - d_{ac} C A - d_A A. \quad (2.11)$$

Despite adding components for AHL degradation, the model of the system's major events does not change significantly. Eq. (2.7) becomes (2.11) with the addition of one term reflecting the new per cell AHL degradation rate caused by the expression of *aiiA* in each cell in the system. d_{ac} ($mL \cdot hr^{-1}$) is arbitrarily modifiable by the experimenter by changing the concentration of the *aiiA* inducer DHBA. The first order AHL degradation term does not go away. AHL will passively degrade in every environment; we have just added enzymatic degradation on top of that breakdown rate.

Our model of *cap and release* indicates that degradation of every species in the circuit: cell-internal proteins, nucleic acids and cell-external AHL signals, is required to realize the circuit's steady state control function. Cell division and intracellular turnover dilute and degrade all internal cell components like transcription factors/toxins and nucleic acids, but AHL signals are only degraded by either environmental or enzymatic degradation. We simulated the effects of degradation on population capping behavior to understand how both kinds of degradation affect the steady state control performance of the *cap and release* system.

We find that AHL degradation is necessary to allow culture growth at all. When k_A is non-zero, but d_A is zero, AHL signals accumulate to high concentrations and activate *ccdB* expression to an extent that the entire population is killed (Fig. 2.9). Increasing d_A allows the establishment of progressively higher population steady states, as AHL no longer accumulates to infinity. At the same time as it increases population steady states, increasing d_A decreases the population's settling time to steady state,

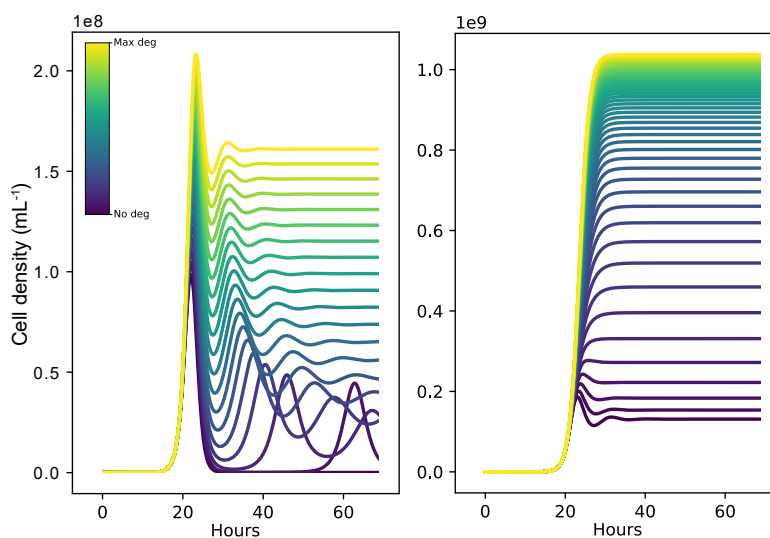


Figure 2.9: Simulating population capping with AHL degradation (LEFT) Simulation of population capping with various rates of passive AHL breakdown, d_a , against k_a of $5 \cdot 10^{-7}$. d_A covers values from 0 to $0.891 \text{ nM} \cdot \text{hr}^{-1}$, the value inferred from data in [52]. (RIGHT) Simulation of population capping subject to various levels of *aiiA* enzyme induction against k_a of $5 \cdot 10^{-7}$; because environmental breakdown is always present, we simulate enzymatic degradation on top of passive environmental breakdown at d_A of $0.891 \text{ nM} \cdot \text{hr}^{-1}$. Settling time is significantly reduced compared to environmental breakdown alone (lowest, purple curve)

demonstrating the trend that faster signal degradation increases population controller speed. Luckily, AHL breakdown will always occur at some rate (meaning d_A is non-zero), but that rate may be too slow in some environments to set population steady states in a reasonable amount of time, necessitating active degradation like we have implemented with *aiiA*. Simulating active enzymatic degradation (increasing d_{ac}) against a background of positive d_A , we see that active enzymatic degradation is able to reduce overshoot and population settling time. AHL degradation trades dynamic range of population capping for controller speed; increasing AHL degradation rate reduces the maximum possible AHL concentration at steady state, setting a lower bound on the population capping performance of the system.

As we can see from the updated model, this new *cap and release* design has many more parameters than the base *pop cap* architecture, each of which will need to be set somewhere in the range of values that allows the circuit to function. To give ourselves the best chance of finding well-performing circuit designs, we chose to build a large pool of circuit variants covering a large amount of parameter space, then screen for improved performance.

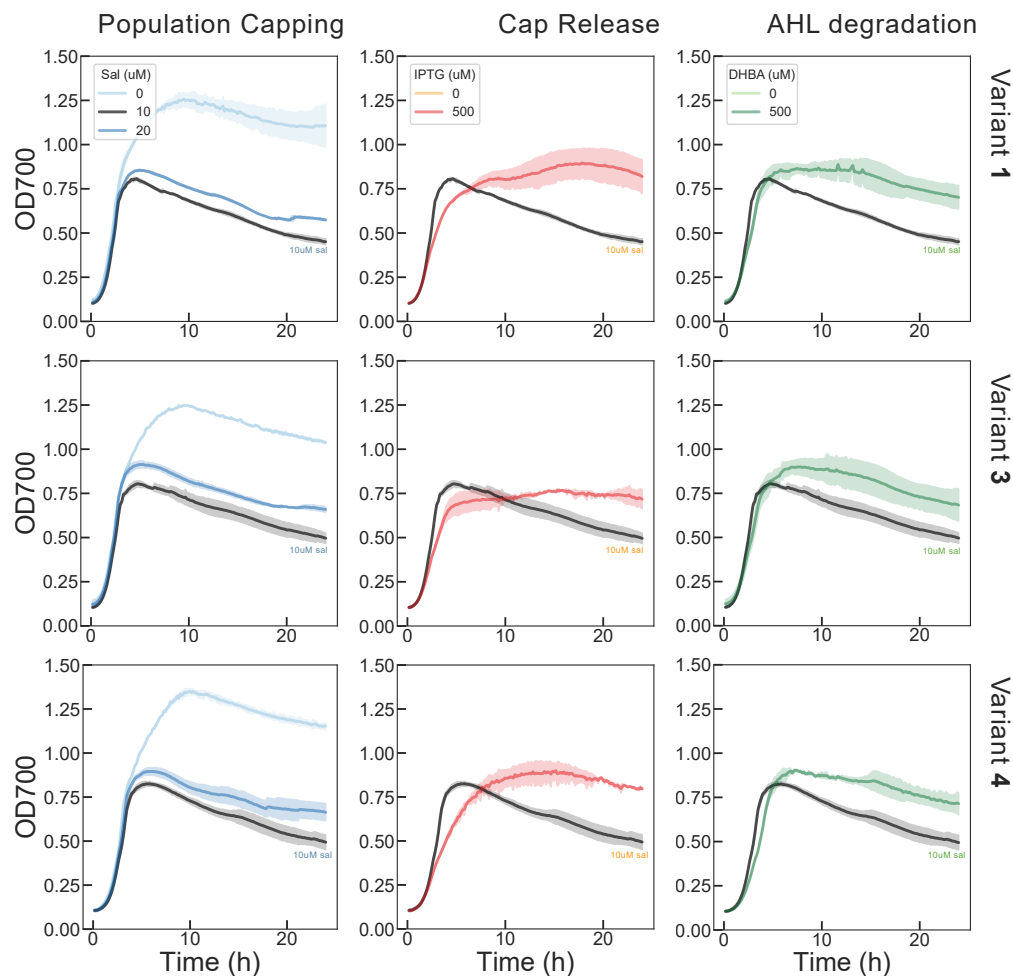


Figure 2.10: Screening *cap* and *release* variants. 3 variants of the *cap* and *release* circuit rebuild exhibiting population capping, cap release and AHL degradation. Curves are the average of 3 replicates, shaded areas represent standard deviation. The maximally capped populations (achieved at 10uM sal in each case) are colored black on each plot to identify density baseline curves that are shared across rows.

The *ccdB* protein is a highly potent toxin and slight overexpression can very easily lead to total population death. As such, the parameter ranges in which this circuit design is actually functional are tight. Previous models and experiments demonstrate that *ccdB* expression rate can be varied to search functional space in this population capping architecture [77]. Using 3G assembly [12], we built the pool of variants with different ribosome binding site (RBS) strengths providing different *ccdB* translation rates to search the widest range of circuit functional space. All other circuit components were designed to be expressed with hardcoded intermediate strength.

Our design goal was a circuit with a large difference in density between capped and uncapped states, the ability to release a population cap, and a density increasing effect

of AHL degradation. We screened the pool of variants by growing each in coarse gradients of population capping inducer, release inducer and degradation inducer (all combinations). Those variants unaffected by the presence of the circuit plasmids (no growth defect at zero inducers) with significant population capping activity, cap release potential and cap interruption by AHL degradation were considered candidate variants for further testing. The screen was conducted in LB medium to optimize this circuit's performance in a more standard bacterial growth medium, rather than the specialized TBK medium used in the original publication of the *pop cap* circuit. The most successful variants demonstrated all three of these behaviors in standard LB medium with significantly increased dynamic range compared to our previous circuit builds (Fig. 2.10).

Each of the tested variants performed very similarly in the screen. Population capping by all three variants (Fig. 2.10, LEFT column) was much more significant than previously demonstrated (capping inducer is now Sal, where it was IPTG before); each variant was capped to an OD700 of ~ 0.5 ($\leq 50\%$ of uncapped density) at 10 μM Sal. Increasing Sal concentration beyond 10 μM does not decrease population cap, instead it appears to cap the populations slightly less strongly. These capped populations also slowly decrease in density after their growth stops at around 5 hours into the experiment. Because maximum population capping was produced by 10 μM Sal, this curve is set as the baseline for visualizing the effects of cap release and AHL degradation (Fig. 2.10, MIDDLE and RIGHT columns).

When *ccdA*-mediated cap release was induced (this time with IPTG), variants 1 and 4 were released most significantly from their caps (Fig. 2.10, MIDDLE column). Cap release also appeared to ameliorate the progressive decline in population density after the arrest of growth at 5 hours. AHL degradation also had the expected steady state density increasing effect on capped cultures, again variants 1 and 4 responded more strongly than did variant 3 (Fig. 2.10, RIGHT column). Degradation did not prevent the slow decline in population density after growth arrest at 5 hours. These results suggest that this slow decline in density is a phenomenon mediated by *ccdB*; only in populations with induction of *ccdB* sequestration is this phenomenon absent.

We chose to make more detailed experiments with variant 4 (Fig. 2.11):

1. Test a very fine gradient of degradation inducer concentrations to visualize effects of degradation on population cap.

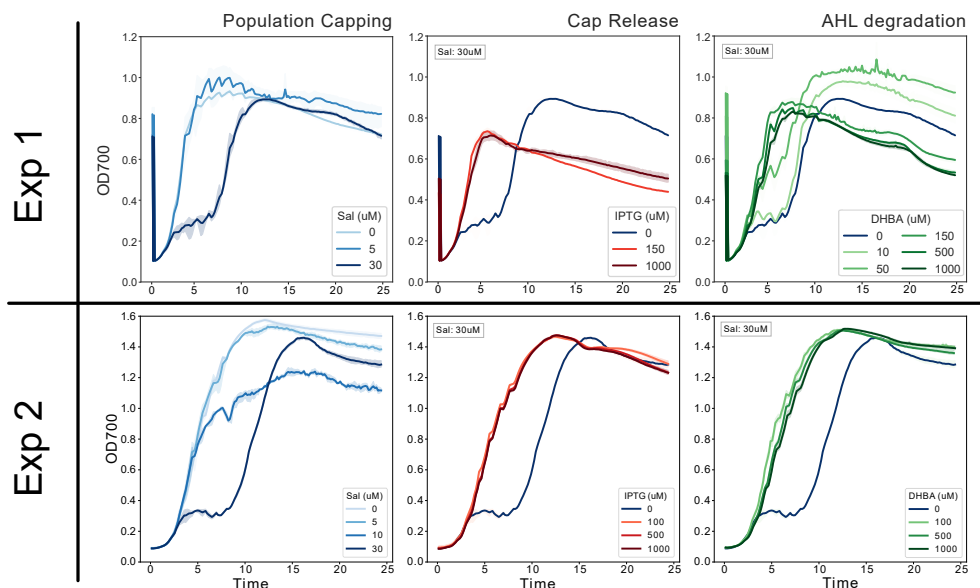


Figure 2.11: Testing *cap* and *release* variant 4 Cultures expressing *Cap* and *release* variant 4 were used in two experiments. The plots presented demonstrate the 3 independent functions of the circuit design, population capping, rescue from capping, and cap interruption with AHL degradation. The curve corresponding to population capping at 30 μ M Sal is colored dark blue in all plots to highlight the baseline from which release and degradation begin.

2. Test finer gradients of *all* component inducers, this time counting CFUs every hour to allow a detailed, dynamic comparison between absorbance-based optical density measurements and viable CFU counts.

Unfortunately, CFU counting for the second experiment is still in progress and the time course comparison between both measurement types is unavailable.

Variant 4's performance differed between each of its experiments (Fig. 2.11). In both experiments with variant 4, 30 μ M Sal produced the most significant population cap, but at 8 hours after the start of *both* experiments, these heavily capped populations exhibited the same cap "escape" behavior previously seen when provoking artificially strong population caps in the base *pop cap* circuit (Fig. 2.3, D-F).

In experiment 1 (Fig. 2.11 TOP), 30 μ M Sal briefly arrested population growth at OD 0.3, but the culture escaped control at 8 hours and grew to match the density of the uncapped population. *ccdA*-mediated release from the 30 μ M Sal cap was incomplete; regardless of *ccdA* induction strength, the population was released to an intermediate density below the uncapped culture's density. AHL degradation produced a variety of different phenotypes: with zero or little degradation against 30 μ M Sal capping, populations were still arrested at low density, then escaped to

high density. With stronger degradation against the 30 μ M Sal cap, populations grew to stable densities below uncapped density; even strong degradation did not allow the cultures to grow to uncapped culture density.

In experiment 2 (Fig. 2.11 BOTTOM), population capping was similar to experiment 1: 30 μ M Sal strongly capped population density, but the culture escaped control after 8 hours. However, in this experiment, only *complete* cap release was observed with increasing induction of *ccdA* and AHL degradation. With any induction of *ccdA* or AHL degradation, the growth arrest produced by 30 μ M Sal was completely ameliorated and the cultures grew as if uncapped.

These two experiments complicate our understanding of *cap and release* circuit function. Before rebuilding the circuit in the form presented in Fig. 2.8, population capping and cap release were reliably produced with their associated inducers, but the effects on population density were small (caps to 75% of uncapped density as measured by OD600, to 30-50% uncapped density as measured by viable cell counts). After building *cap and release* with AHL degradation and screening variants for cap, release and degradation functions, the effects of each function on population density are much more dramatic, but also variable between experiments.

These data demand further experimentation with *cap and release* to test a few hypotheses:

- **Stronger population capping decreases the evolutionary stability of circuit function:**

In experiments 1 and 2, strong population capping arrests growth at a dramatically low density, even when measured using OD700, which overestimates viable cell counts. This growth arrest does not produce a stable population cap; these arrested cultures eventually begin growing again to meet the density of uninduced populations. Less significant inductions of population capping do not demonstrate this "escape" behavior (Fig. 2.10). It is possible that by increasing the population capping power of *cap and release*, we have reached a limit of function at which the growth burden imposed by population capping is so significant that mutants inactivating the circuit are quickly selected and dominate the population. This possible failure mode is not new to synthetic biologists or circuit architectures of this type [64]. Metagenome sequencing of the *cap and release* plasmids in "escaped"

cultures will reveal whether mutation of circuit components is responsible for this phenomenon.

- **Experimental setup alters circuit function:**

The road to performing the variant screen and Experiments 1 and 2 is paved with *cap and release* experiments that failed to demonstrate any kind of population control. The difference between those "failures" and the screen/Experiments 1 and 2 lies in the preparation of the cells for experimentation. We find that cells simultaneously transformed with the *cal* and *pLuxARLccdB* plasmids—a standard co-transformation—never exhibit population control in experiments. Cells sequentially transformed with *cal* plasmid, then *pLuxARLccdB* are more likely to exhibit *cap and release* functions. However, even sequentially transformed cells seem to lose circuit function after extended outgrowth for experimentation. The standard overnight outgrowth before an experiment nearly always renders a *cap and release* cell line incapable of population control.

In the variant screen and Experiments 1 and 2, the cell lines are freshly sequentially transformed with *cal*, then *pLuxARLccdB* plasmids. To avoid overnight culture, these transformants are inoculated into outgrowth medium, then grown only until they reach OD600 ~0.3, then immediately aliquoted into an experiment.

This process minimizes two things: unprotected exposure of cells to ccdB and time under circuit burden. The *cal* plasmid contains the ccdA antitoxin and is expected to "leak" a small amount of ccdA protein even without induction of its expression. Transforming cells with this plasmid first creates an intracellular environment in which normally lethal "leak" of ccdB from the *pLuxARLccdB* plasmid is sequestered by ccdA, allowing cells harboring both plasmids to grow and participate in experiments.

As a population control circuit actuated by a lethal toxin, *cap and release* is designed to impose an extreme burden on cells. The longer this burdensome circuit remains in a cell, the more likely it is to acquire an inactivating mutation. If this mutation inactivates ccdB expression, that mutant is very likely to survive and dominate the population, especially during an experiment during which *non*-mutants are induced to cap their own growth. Overnight growth before an experiment provides a long growth period during which mutations can accumulate and prevent circuit function in a later experiment. Short outgrowth before an experiment hopes to minimize

the possibility of mutating our circuit before it is tested. Experiments comparing outgrowth time to population control function may help us measure how long it takes for inactivating mutations to appear.

It will be critical to continue testing *cap and release* cell lines created and prepared for experimentation with identical procedures to determine how much circuit variability is simply due to stochasticity in circuit function, and how much is due to variation in experiment preparation.

2.3 Discussion

Expanding on the 2004 *pop cap* genetic circuit that imposes a density cap on a population of bacteria using AHL signal feedback and *ccdB* toxin expression, we designed and built the *cap and release* circuit, which adds new population control functions to allow complex population density control and scaling to more complex heterogeneous controlled communities. With its multiple inputs and bidirectional actuators on population density, the *cap and release* circuit can serve as a basic motif for designing more complex multi-strain genetic circuits. One such circuit is the $A=B$ circuit, discussed in the following chapter of this thesis.

In the process of building the *cap and release* circuit, we created modular genetic parts for the *ccdB*, *ccdA* and *aiiA* proteins (available along with all the other parts of this circuit in Addgene Kit 1000000161 "CIDAR MoClo Extension, Volume I").

Two major directions remain to be explored in validating this circuit design. First, the *aiiA* protein is shown to degrade AHL effectively in this circuit, which is predicted to decrease its recovery time after perturbation. Experiments need to be done to verify this model prediction. All presented experiments in this work allow circuit-containing communities to grow to steady state density in a single growth phase without dilution or addition of additional cells. Making these perturbations to a steady system and tracking its recovery by counting viable colonies will be critical to validate *aiiA* as an improvement to the original *pop cap* circuit design.

Secondly, The original population capping circuit was designed to function by exploiting variability in circuit component expression among population members. The authors used *lacZ*-tagged *ccdB* to measure bulk circuit output in the population, but did not measure the *distribution* of *lacZ*-*ccdB* expression among single cells in the population. Where a simple differential equation model of population capping allows a continuous relationship between *ccdB* toxin expression and aggregate population death rate, the reality of this circuit is much noisier and more discrete. Each

individual cell will produce different amounts of *ccdB* toxin in response to Lux AHL due to noisy expression of all its circuit components. Again stochastically, not every cell will die at an identical intracellular concentration of *ccdB*.

To truly understand how this population capping works, we need to investigate the role of noise in circuit function. To learn about the related distributions of *ccdB* expression and cell viability, we have tagged *ccdB* with GFP and plan to use flow cytometry to measure the distribution of GFP-*ccdB* fluorescence along with the distribution of a live/dead cell dye (like the Invitrogen LIVE/DEAD BacLight dye). We suspect that the live cells counted in CFU assays are those on the low end of GFP-*ccdB* expression. These results will clarify the exact mechanisms underlying population capping in this genetic circuit. Stochastic, population level simulation software developed in our laboratory also allows us to model this mechanism and compare data to predictions to assess the validity of our hypothesis [78].

2.4 Materials and Methods

E. coli cell strains

DH5 α Z1 *E. coli* were used to create the *pop cap* strain used in this work. DH5 α Z1 *E. coli* were also used to create the *cap and release* strain containing (*ccdA/ccdB*) toxin sequestration; strain CY027 [79] was used to create the *cap and release* strain containing RNA-level *ccdB* sequestration. Both strains have genome integrations expressing the necessary activator/repressor transcription factors to allow regulated expression of circuit components: DH5 α Z1 has genome integrated expression of LacI and TetR; C027 has genome integrated expression of both RhIR and CinR.

The Marionette Wild (*E. coli* MG1655 base) strain [34] was used to create the rebuilt *cap and release* variants (Fig. 2.4). It contains a genome integrated cassette that expresses 12 different transcription factors allowing gene regulation in response to 12 inducers, including those we use in this work (IPTG, Sal, DHBA and Lux AHL).

DB3.1 *ccdB*-resistant *E. coli* were used to amplify and purify *ccdB* containing *pLuxARLccdB* plasmids. These cells contain the mutant *gyrA462* DNA gyrase, rendering them resistant to *ccdB* toxicity. DB3.1 cells were obtained from the Belgian Co-ordinated Collections of Microorganisms, accession number LMBP 4098. DB3.1 was originally sold by Invitrogen, but has been discontinued as a product.

As mentioned in the text, the method of preparing *cap and release* cell lines is specifically designed to minimize loss of circuit function in the resulting cells.

Whenever a strain must be transformed with plasmids containing the *ccdB* toxin and a toxin sequestration mechanism, the base strain should be transformed first with the plasmid containing the toxin sequestration element. This singly transformed cell line should then be prepared for transformation a second time with the *ccdB* containing plasmid. This process avoids exposing cells to leaky *ccdB* expression without protection with a sequestration element.

Plasmids

The *pop cap* circuit is composed of two plasmids: *pLuxRI2*, *pluxCcdB3* (both from [52])

The *cap and release* circuit with *ccdA/ccdB* sequestration contains 3 plasmids: *pLuxRI2*, *pluxCcdB3* (both from [52]), and *pTetCcdA*.

pTetCcdA was constructed by GoldenGate assembly of (promoter-RBS-CDS-terminator):

pTet - B0033m - *ccdB* - B0015 terminator

into a *pSC101* backbone containing carbenicillin resistance. The *ccdB* coding sequence was taken from the *pOSIP_KO* plasmid [80]

The *cap and release* circuit with RNA-level (RNA-IN/RNA-OUT) toxin sequestration contains 3 plasmids: *pRNAINccdB*, *pRNAOUT* and *pRhII*.

pRNAINccdB was constructed by Gibson assembly of (promoter-RBS-CDS-terminator):

pRhI - RNA-IN module [69] - *ccdB* - B0015 terminator

into a *p15a* backbone containing chloramphenicol resistance.

pRNAOUT was constructed by Gibson assembly of

pCin - RNA-OUT

into a *ColE1* backbone containing kanamycin resistance.

pRhII was constructed by Gibson assembly of:

J23106 promoter - B0034 - *lacI* - B0015 terminator;

pLac - B0034 - *rhII* - B0015 terminator

together into a *pSC101* backbone containing carbenicillin resistance.

Rebuilt *cap and release* variant plasmids with *aiiA* degradase were constructed using the following parts, by the 3G assembly method [12]. The specific constructs are

detailed below in the format (promoter - ribosome binding site - CDS - terminator / ...):

cal:

pTac [34] - BCD8 - ccdA - ECK120033736 /

pCauAM [34] - B0032 - aiiA - L3S2P11 /

pSalAM [34] - B0032 - LuxI - B0015

into plasmid with ColE1 origin of replication, kanamycin resistance.

pluxARLccdB:

pLuxAM [34] - ARL (see link below) - ccdB - B0015

(Link: [ARL ribosome binding site library](#))

into a plasmid with pSC101 origin of replication, chloramphenicol resistance

Unless otherwise noted, all parts used in cloning can be found in the Murray Lab Parts Library (Addgene Kit 1000000161 "CIDAR MoClo Extension, Volume I").

Cell Growth Experiments

Cells containing *pop cap* or *cap and release* were grown from a *freshly transformed* colony (see recommendations under "*E. coli* cell strains") in either LB or TBK medium (10g tryptone, 7g KCl per liter, 100mM MOPS buffer) to an OD600 of 0.3 in medium matching the medium used in the experiment.

These low density outgrowths were then diluted 10x into fresh medium with the appropriate antibiotics (carbenicillin (100 μ g/mL), kanamycin (50 μ g/mL) and chloramphenicol (25 μ g/mL)) and aliquoted in triplicate in 500uL into a square 96 well Matriplate (dot Scientific, MGB096-1-1-LG-L) pre-loaded with chemical inducers. Inducers were added to the 96 well Matriplate before cell suspensions were aliquoted. A Labcyte Echo 525 Liquid Handler was used to aliquot inducers, with the exception of DHBA, into each well of the plate before cell suspensions were added. DHBA is dissolved in ethanol, which is not accurately pipetted by the Echo 525; DHBA was input into plates by hand.

The plate was incubated for the duration of the experiment in a Biotek Synergy H2 incubator/plate reader run by the Gen5 software. Temperature was set to 37°C, shake setting was the maximal rate of *linear* shaking.

OD600/OD700 measurements were taken every 10 minutes. If samples were taken for CFU counting, plates were ejected from the plate reader, 10uL of culture was aliquoted into 30uL of 20% glycerol (15% final glycerol concentration); this glycerol suspension was frozen at -80°C for later colony counting.

Cell Density Quantification

Colony forming units were counted using two methods:

Droplet CFU counting: Cell suspensions were diluted 25,000x into fresh TBK media and aliquoted into a Labcyte Echo 384 well source plate. 50nL drops of this suspension were transferred to regions on a Nunc OmniTray (ThermoFisher: 140156) filled with LB agar containing the appropriate antibiotics. The OmniTray was incubated at 37°C overnight, then colonies were counted. The fraction of droplets spotted on the plate that DID NOT grow colonies was fit to a Poisson distribution to determine λ , which yielded the mean cells/mL.

Plate CFU counting: Cell suspensions were diluted between 10 - 10⁶x into fresh LB medium, then 10uL of this suspension was spread on LB agar petri dishes. These plates were incubated at 37°C overnight, then colonies were counted. The number of colonies grown was multiplied by the dilution factor (and the 4x dilution factor that occurred during sampling) to obtain cells/mL.

Modeling and Simulations

The variables in the presented models are as follows:

C: cell density ($\frac{cell}{mL}$)

T: CcdB concentration (nM)

R: Sequestration device concentration (nM)

A: AHL concentration (nM)

Parameters in the model:

k_c : cell growth rate constant (0.897 hr^{-1}) [52]

C_{max} : carrying capacity for cell growth ($1.16 * 10^9 \text{ ml}^{-1}$) [52]

β : cooperativity of AHL effect ($\beta = 2$)

d_c : cell death rate constant by ccdB ($4 * 10^{-3} \text{ nM}^{-1} \cdot \text{hr}^{-1}$) [52]

k : concentration of AHL to half-maximally active promoter (100 nM) [81]

k_{on} : binding rate of ccdB and sequestration device ($3 \text{ nM}^{-1} \cdot \text{hr}^{-1}$)

g_R : basal production rate of sequestration module; modifiable by experimenter ($0 - 10 \text{ uM} \cdot \text{hr}^{-1}$)

k_T : synthesis rate constant of CcdB ($5 \text{ nM} \cdot \text{hr}^{-1}$) [52]

k_A : synthesis rate constant of AHL ($4.8 \times 10^{-7} \text{ nM} \cdot \text{ml} \cdot \text{hr}^{-1}$) [52]

d_A : decay rate constant of AHL ($0.891 \text{ nM} \cdot \text{hr}^{-1}$) [52]

d_T : decay rate constant of ccdB toxin (2 hr^{-1}) [52]

d_{ac} : per cell AHL degradation rate by aiiA (true value unknown, varied in simulations, $\text{mL} \cdot \text{min}^{-1}$)

Parameter estimates were found in multiple literature sources [52, 58]

2.5 Supplementary Material

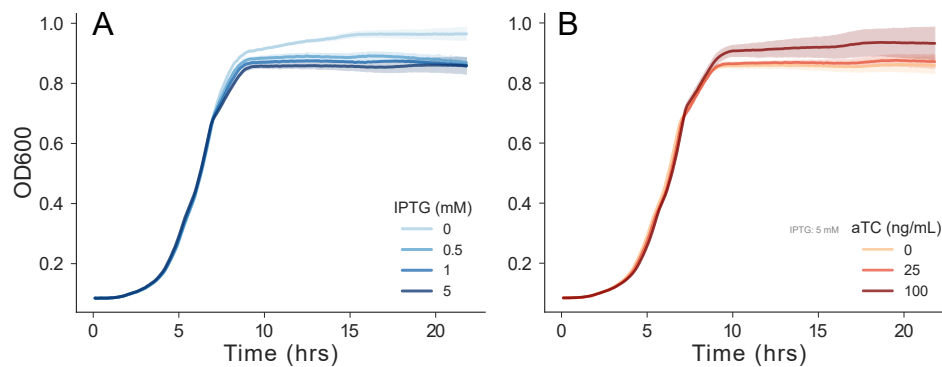


Figure 2.12: Additional testing of *cap* and *release* An additional experiment with *cap* and *release* employing the ccdB/ccdA protein-level sequestration module. At the end of this experiment, samples were taken to measure viable cell counts. Data from this counting is presented in Fig. 2.7